ATMOSPHERIC AND OCEANIC SCIENCE LETTERS, 2015, VOL. 8, NO. 6, 358–364

Revisiting Mid-Holocene Temperature over China Using PMIP3 Simulations

TIAN Zhi-Ping[1] and JIANG Da-Bang[1,2]

[1] *Climate Change Research Center, Chinese Academy of Sciences, Beijing 100029, China*
[2] *Nansen-Zhu International Research Centre, Institute of Atmospheric Physics, Chinese Academy of Sciences, Beijing 100029, China*

Received 28 April 2015; revised 17 June 2015; accepted 26 June 2015; published 16 November 2015

Abstract Using the simulations performed by 15 climate models under the latest protocol of the Paleoclimate Modeling Intercomparison Project (PMIP) Phase 3 (PMIP3), the authors revisited the annual and seasonal temperature changes over China during the mid-Holocene. Similar to the previous results produced by PMIP Phase 1 (PMIP1) and 2 (PMIP2) models, 14 (15) of the 15 PMIP3 models reproduced colder annual (boreal winter and spring) temperature in response to mid-Holocene insolation changes, with an average cooling of 0.33 K (1.31 K and 1.58 K) over China. The mid-Holocene boreal summer (autumn) temperature increased in all (13) of the 15 PMIP3 models, with an average warming of 1.02 K (0.61 K) at the national scale. Those changes simulated by the PMIP3 models were similar to those from the PMIP2 simulations but generally weaker than those from the PMIP1 models. A considerable mismatch still existed between the simulated cooling by the PMIP3 models and the reconstructed warming for annual and winter temperatures over China during the mid-Holocene, as was also the case between the previous PMIP1/2 simulations and proxy data.

Keywords: Mid-Holocene, temperature over China, PMIP3 simulations

Citation: Tian, Z.-P., and D.-B. Jiang, 2015: Revisiting mid-Holocene temperature over China using PMIP3 simulations, *Atmos. Oceanic Sci. Lett.*, **8**, 358–364, doi:10.3878/AOSL20150040.

1 Introduction

The mid-Holocene, 6000 years before present, was a period when the climate and environment were remarkably different from today (Bartlein et al., 2011), mainly due to a change in incoming solar radiation at the top of the atmosphere (Berger, 1978). It is an ideal time period for investigating past climate change on the orbital scale, for which proxy data are abundant and relatively reliable. The mid-Holocene is also one of the benchmark periods within the framework of the Paleoclimate Modeling Intercomparison Project (PMIP), in which a hierarchy of climate models simulate the mid-Holocene climate either at the global (e.g., Braconnot et al., 2007; O'ishi and Abe-Ouchi, 2011) or regional scale over the monsoon regions of northern and southern Africa, North and South America, and northern Australia (e.g., Joussaume et al., 1999; Liu et al., 2004; Zhao and Harrison, 2012). Comparatively, however, less emphasis has been placed on the East Asian monsoon region (e.g., Wang et al., 2010; Zhou and Zhao, 2010, 2013), and thus there is an urgent need to further investigate the mid-Holocene East Asian climate.

Numerous efforts have been devoted to reconstructing the mid-Holocene climate over East Asia using a variety of proxy data, which suggest China experienced generally warmer and wetter than present conditions during that time. By contrast, some simulations focused on the mid-Holocene summer (June–August) climate over East Asia have been performed using atmospheric general circulation models (AGCMs) (e.g., Wang, 1999, 2002; Wang and Wang, 2013), regional climate models nested within AGCMs (e.g., Zheng et al., 2004), atmosphere-ocean general circulation models (AOGCMs) (e.g., Wei and Wang, 2004), and atmosphere-ocean-vegetation general circulation models (AOVGCMs) (Dallmeyer et al., 2010). In these previous studies, a warmer summer climate and stronger monsoon circulation over East Asia during the mid-Holocene have been reasonably reproduced, but there is a large degree of uncertainty among simulations. Additionally, little attention has been paid to the climate change for the annual mean and the other three seasons.

Recently, Jiang et al. (2012) examined annual and seasonal temperatures over China during the mid-Holocene using 36 climate models, including 16 AGCMs in PMIP Phase 1 (PMIP1) and 20 coupled models in Phase 2 (PMIP2). They found that 35 (36) of the 36 models reproduced colder-than-baseline annual (winter, December–February) temperature over China during that time—opposite to the warmer-than-present conditions derived from multiple proxy data sources. Similar results were obtained from the median of 10 PMIP Phase 3 (PMIP3) models (Zheng et al., 2013) and a state-of-the-art AOVGCM (Tian and Jiang, 2013). Furthermore, Jiang et al. (2012) and Liu et al. (2014) pointed out that the uncertainties in both PMIP simulations and proxy data may be responsible for the above model-data mismatch, in which quite different performances were found between PMIP1 AGCMs and PMIP2 coupled models, and different results could be interpreted from the reconstructed records with sparse spatial coverage. Considering that only the PMIP1/2 models and some PMIP3 models have been used in these earlier studies for the mid-Holocene climate over China, as well as the identified model-dependent uncertainties in the simulations, all available models of the latest PMIP3/

Corresponding author: TIAN Zhi-Ping, tianzhiping@mail.iap.ac.cn

Coupled Model Intercomparison Project Phase 5 (CMIP5) simulations need to be revisited and compared to multiple proxy data, in order to try uncover some clues about whether the inconsistency between the simulated cooling and reconstructed warming of the mid-Holocene annual and winter climates over China arises from the models, from the proxy data, or from both sides.

2 Data

2.1 Models and data

The present study was based on all 15 of the climate models under the latest PMIP3/CMIP5 protocol for mid-Holocene climate simulations, including eight AOGCMs and seven AOVGCMs, which have overall higher horizontal resolution than the former PMIP1/2 models. Basic information on the 15 models is provided in Table 1. The boundary conditions for the mid-Holocene experiment included changes in the Earth's orbital parameters (Berger, 1978), which played the most important role in the mid-Holocene climate, and atmospheric greenhouse gas concentrations. In PMIP3, the atmospheric concentrations of CO_2, CH_4, and N_2O varied from the pre-industrial (baseline) levels of 284 ppm, 791 ppb, and 275 ppb, to 280 ppm, 650 ppb, and 270 ppb during the mid-Holocene, respectively. Sea surface temperatures (SSTs) were computed by oceanic general circulation models, and the vegetation was fixed at the present state in AOGCMs but was simulated with dynamic vegetation models in AOVGCMs for both the baseline and mid-Holocene experiments. More details about the models and experiments are provided by Taylor et al. (2012).

The temperature data used for model evaluation were taken from the CN05.2 monthly dataset for the period 1961–2000, with a half-degree horizontal resolution over China, provided by the National Climate Center of the China Meteorological Administration (Wu and Gao, 2013). Given that there are differences in the horizontal resolution among the models, all model and observational data were aggregated to a relatively mid-range resolution of 2.5° × 2° (longitude × latitude).

2.2 Evaluation of climate models

Whether or not the climate models can reasonably reproduce the present annual and seasonal temperature climatology over China, both in pattern and magnitude, will largely determine the confidence we have in their results for the mid-Holocene climate. In this sense, the spatial correlation coefficient (SCC), standard deviation, and centered root-mean-square difference (CRMSD) of each baseline experiment with respect to observation were calculated based on 179 grid points across mainland China. As shown in the Taylor diagram (Fig. 1), the SCCs ranged from 0.86 to 0.99 for annual and seasonal temperatures, all of which were statistically significant at the 99% confidence level, indicating reliable performance of

Table 1 Basic information about the 15 climate models within PMIP3 for the mid-Holocene experiments used in this study.

Numbers	Model ID	Model full name	Model type	Atmospheric resolution	Length of run analyzed (year)
01	BCC-CSM1.1	Beijing Climate Center Climate System Model version 1.1	AOVGCM	~2.8° × 2.8°, L26	100
02	CCSM4	Community Climate System Model version 4	AOGCM	1.25° × ~0.9°, L26	301
03	CNRM-CM5	Centre National de Recherches Météorologiques-Coupled Model version 5.1	AOGCM	~1.4° × 1.4°, L31	200
04	CSIRO-Mk3-6-0	Commonwealth Scientific and Industrial Research Organization Mark 3.6 climate system model	AOGCM	1.875° × ~1.9°, L18	100
05	CSIRO-Mk3L-1-2	Commonwealth Scientific and Industrial Research Organization Mark 3 Low-resolution model version 1.2	AOGCM	~5.6° × 3.2°, L18	500
06	EC-EARTH-2-2	European Centre Earth system model version 2.2	AOGCM	1.125° × ~1.1°, L62	40
07	FGOALS-g2	Flexible Global Ocean-Atmosphere-Land System Model Grid-point Version 2	AOVGCM	~2.8° × 3–6°, L26	100
08	FGOALS-s2	Flexible Global Ocean-Atmosphere-Land System model Spectral Version 2	AOVGCM	~2.8° × 1.7°, L26	100
09	GISS-E2-R	ModelE2 version of the Goddard Institute for Space Studies climate model with Russell ocean model	AOGCM	2.5° × 2°, L40	100
10	HadGEM2-CC	Hadley Global Environment Model version 2 Carbon Cycle configuration	AOVGCM	1.875° × 1.25°, L60	35
11	HadGEM2-ES	Hadley Global Environment Model version 2 Earth System configuration	AOVGCM	1.875° × 1.25°, L38	102
12	IPSL-CM5A-LR	Earth System Model of the Institut Pierre Simon Laplace: Low Resolution	AOVGCM	3.75° × ~1.9°, L39	500
13	MIROC-ESM	Earth System Model of Model for Interdisciplinary Research On Climate	AOVGCM	~2.8° × 2.8°, L80	100
14	MPI-ESM-P	Earth System Model of Max-Planck-Institut für Meteorologie: low resolution grid and paleo mode	AOGCM	1.875° × ~1.9°, L47	100
15	MRI-CGCM3	Meteorological Research Institute Coupled ocean-atmosphere General Circulation Model version 3	AOGCM	1.125° × ~1.1°, L48	100

the models in simulating the spatial pattern of the observed temperature climatology over China. Normalized standard deviations (CRMSDs) were 0.95–1.24 (0.26–0.52) for the annual mean, 0.90–1.16 (0.26–0.52) for winter, 0.97–1.44 (0.31–0.71) for spring (March–May), 0.87–1.21 (0.23–0.53) for summer, and 0.96–1.19 (0.21–0.41) for autumn (September–November) temperature. Generally, most models overestimated the spatial variability of annual and seasonal temperatures over China, since their standard deviations were larger than the observed values. They showed their best performance in autumn and poorest performance in spring. Note that most models performed better than PMIP1/2 models for modern temperature climatology, as indicated by their higher SCCs and lower CRMSDs (Jiang et al., 2012). In terms of the median of the 15 models, an SCC of 0.97–0.98, a normalized standard deviation of 1.02–1.14, and a normalized CRMSD of 0.21–0.31 were produced for annual and seasonal temperatures, showing a quantitatively higher reliability than most of the individual models (Fig. 1). Thus, the median of the 15 models is emphasized in the following analysis.

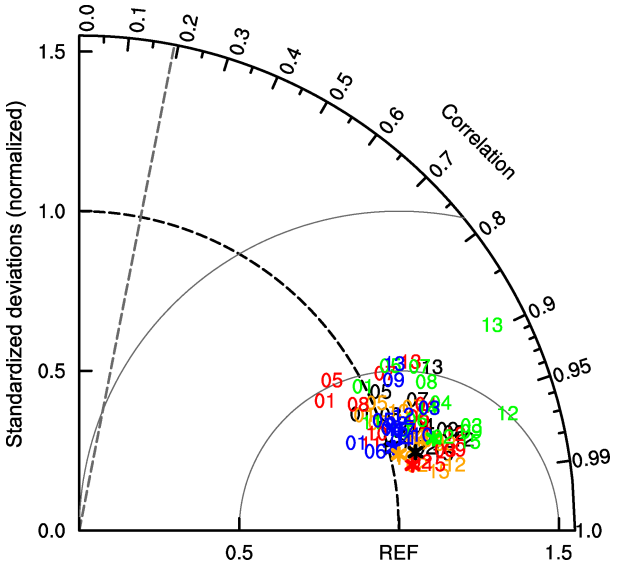

Figure 1 Taylor diagram (Taylor, 2001) displaying normalized pattern statistics of climatological annual (black), winter (blue), spring (green), summer (red), and autumn (orange) temperatures over China between 15 models for the baseline period and observation for 1961–2000. The radial coordinate gives the standard deviation normalized by the observed value, and the angular coordinate gives the correlation with observation, with oblique dashed lines showing the 99% confidence level. The normalized centered root-mean-square difference between a model and observation (marked as REF) is their distance apart. Numbers indicate the models listed in Table 1, and asterisks represent the median of the 15 models.

3 Mid-Holocene temperature over China

3.1 Annual temperature changes

With respect to the baseline period, 14 out of 15 PMIP3 models reproduced colder annual temperatures over China during the mid-Holocene (Fig. 2). Quantitatively, the regionally averaged change over China ranged from −0.97 K (FGOALS-g2; the model full name is provided in Table 1, hereafter the same) to 0.32 K (HadGEM2-ES), with two models (CNRM-CM5 and HadGEM2-CC) showing a very weak cooling of less than 0.1 K and only one model (HadGEM2-ES) indicating a warming. Though it differed somewhat from model to model, the simulated magnitude of annual temperature change was similar to that from the 20 PMIP2 coupled models but generally weaker than that from the 16 PMIP1 AGCMs (Jiang et al., 2012). Considering the median of the 15 models, annual temperature averaged over China was reduced by 0.33 K during the mid-Holocene relative to the baseline period, with a standard deviation of 0.33 K across individual models. The geographical distribution of

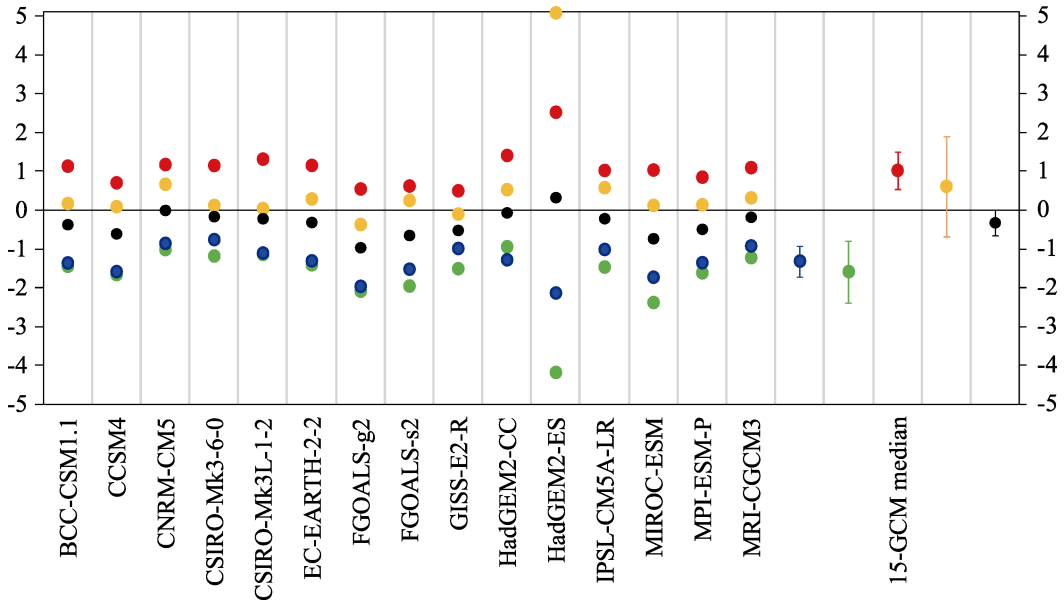

Figure 2 Mid-Holocene–baseline anomalies of regionally averaged annual (black), winter (blue), spring (green), summer (red), and autumn (orange) temperatures over China (units: K) obtained from the 15 models and their median, with plus/minus one standard deviation from the corresponding median expressed by the vertical bars.

the mid-Holocene annual temperature change in the 15-model median showed a generally weak cooling, with a high consistency among the models, over most of China, but a weak warming over northern Northeast China, most of Xinjiang, and part of North and central China (Fig. 3a). Annual temperature change was less than 0.6 K over most of China, except over the eastern Tibetan Plateau and South China where the cooling was 0.6–1.2 K. The spatial pattern of annual temperature change over China simulated by the 15 PMIP3 models was generally similar to the 10 PMIP3 model result in Zheng et al. (2013), but significant cooling was only shown in part of South China and warmer temperature was simulated over most of the Tibetan Plateau, excluding its central part, in the 10-model median (Zheng et al., 2013).

In response to mid-Holocene orbital forcing, SSTs changed significantly with respect to the baseline period according to the 12 models with SST data available (Fig. 4). Annual SSTs generally increased north of 30°N but decreased south of it in the Northern Hemisphere, with the latter change being consistent in most models and thus playing a major role (Fig. 4a). As a result, the consistently colder SSTs in the oceans adjacent to the East Asian continent could lead to larger losses of surface heat over East Asia during warm months and smaller gains of surface heat during cold months, inducing an overall decrease in

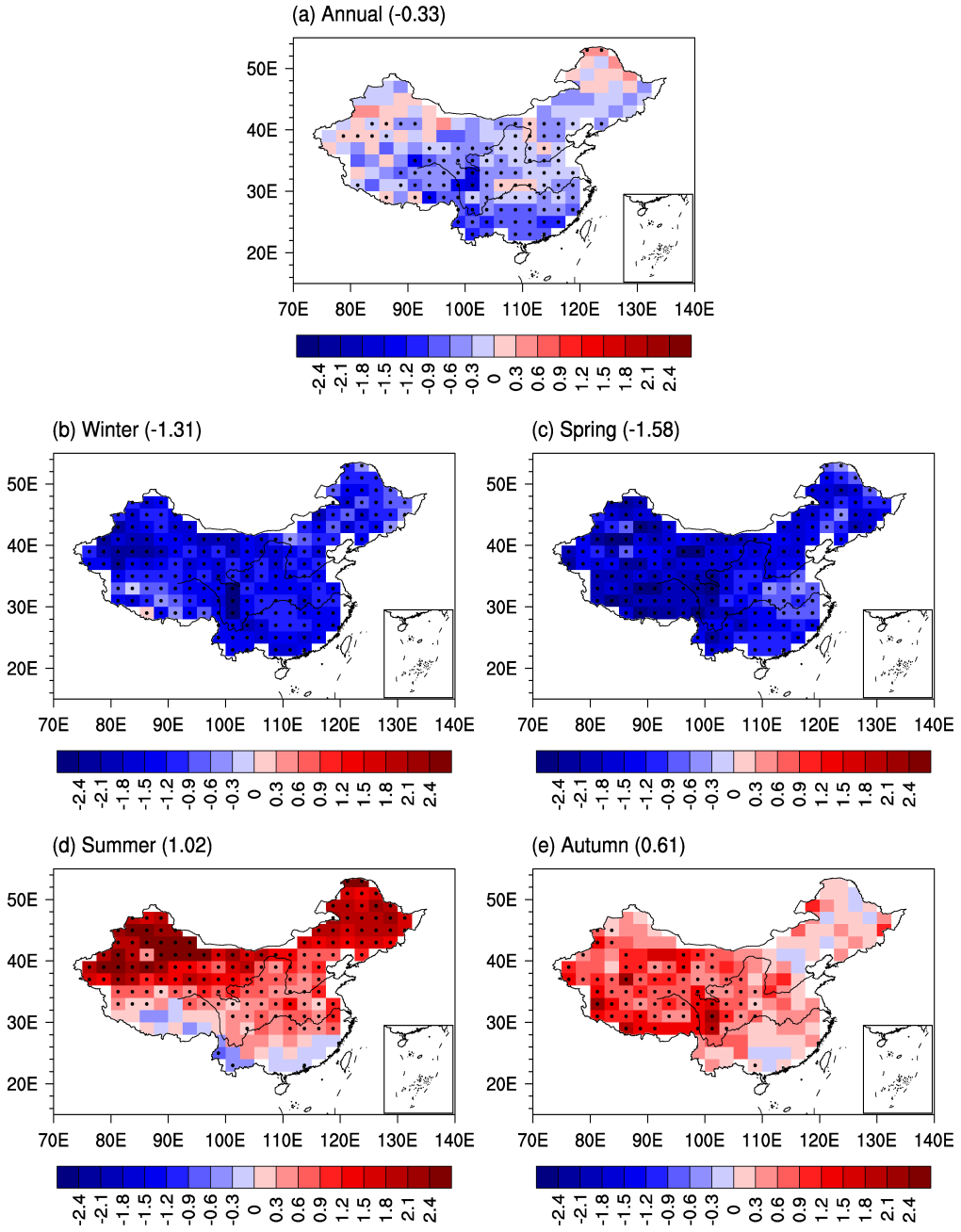

Figure 3 Mid-Holocene–baseline anomalies of annual and seasonal temperatures (units: K) for the median of the 15 models, with regionally averaged values over China given in parentheses. The dotted areas represent regions where at least 80% of the models share the same sign of anomaly.

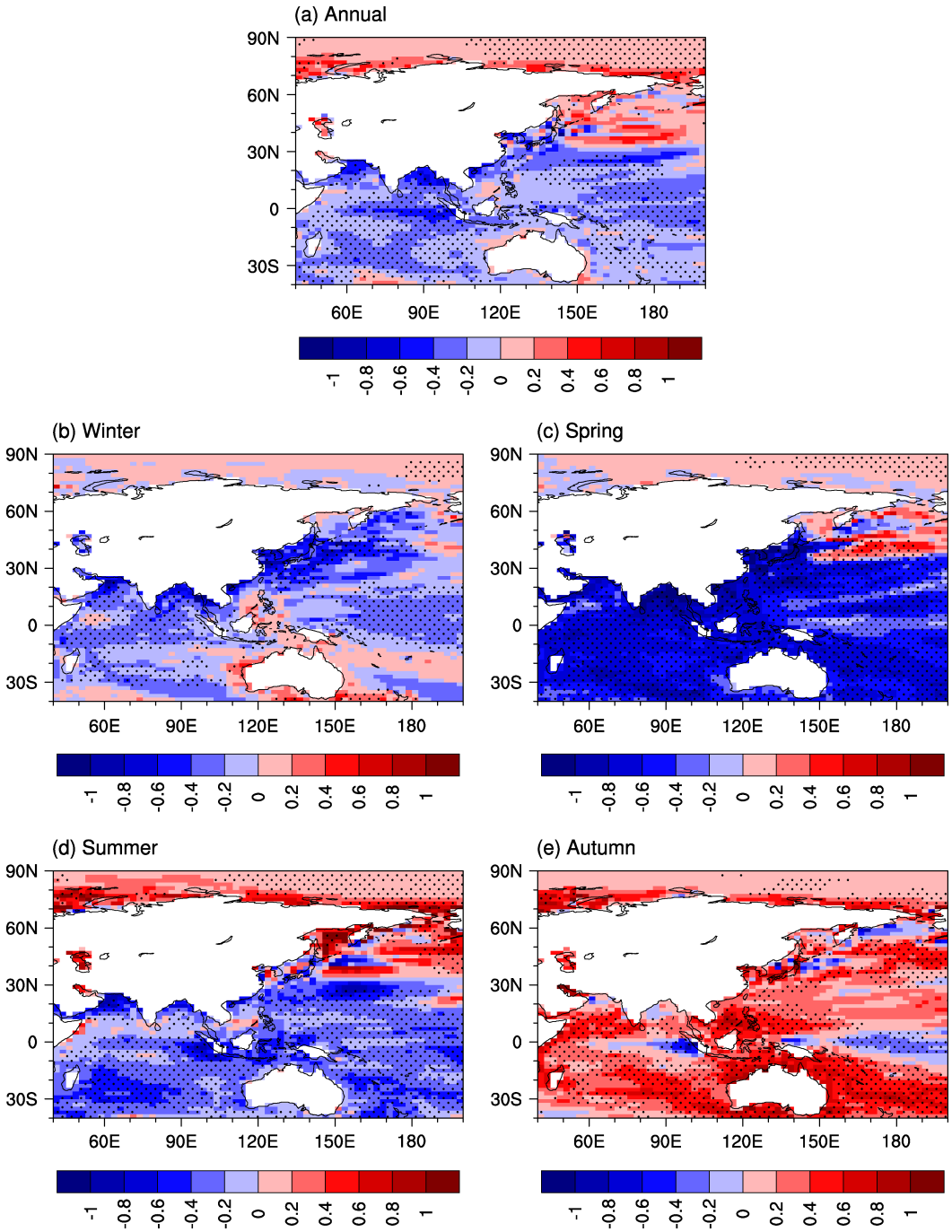

Figure 4 Mid-Holocene–baseline anomalies of annual and seasonal SSTs (units: K) for the median of 12 models (excluding FGOALS-g2, FGOALS-s2, and MIROC-ESM—SST data unavailable). The dotted areas represent regions where at least 80% of the models share the same sign of anomaly.

surface air temperature over China (Fig. 3a).

3.2 Seasonal temperature change

As mentioned in Jiang et al. (2012) and Tian and Jiang (2013), the mid-Holocene change in seasonal temperature generally followed the insolation change over China, which was reduced in winter, spring, and autumn but increased in summer relative to the present day. In response to those changes, all of the 15 PMIP3 models reproduced colder winter and spring temperatures over China during the mid-Holocene, with the national-averaged change ranging from −2.13 K to −0.76 K and from −4.18 K to −0.94 K, respectively (Fig. 2). The median of the 15 models showed a winter (spring) cooling of 1.31 K (1.58 K) averaged over China, with a standard deviation of 0.40 K (0.80 K) across the models. The cooling magnitude (standard deviation) of winter and spring temperatures in the PMIP3 models was comparable to that in the PMIP2 models, but generally smaller (larger) than the PMIP1 AGCM results (Jiang et al., 2012). In summer, temperature increased by 0.50–2.52 K in all of the 15 models averaged over China during the mid-Holocene, with a warming

of 1.02 K in the median of the 15 models. The warming magnitude was quantitatively comparable to that obtained from PMIP1/2 models (Jiang et al., 2012). Autumn temperature over China was increased by 0.04–5.08 K in 13 models but decreased by 0.10 K in GISS-E2-R and by 0.37 K in FGOALS-g2 during the mid-Holocene, with a median warming of 0.61 K and a standard deviation of 1.29 K across the models. Thus, there was a large degree of scatter in the simulated autumn temperature among the PMIP3 models. Note that the overall autumn warming over China did not follow the reduced autumn insolation during the mid-Holocene, which was also the case in the PMIP2 models but opposite to the cooling reproduced by the PMIP1 models (Jiang et al., 2012). This may be because of the different baseline period used in the PMIP1, PMIP2, and PMIP3 models, which was the present day (ca. 1985) in PMIP1 but the pre-industrial period (ca. 1750) in PMIP2/3. It is also worth mentioning that there were large seasonal climate changes during the mid-Holocene in HadGEM2-ES, showing strongest cooling in winter and spring but strongest warming in summer and autumn among the 15 PMIP3 models (Fig. 2). This was because HadGEM2-ES reproduced relatively lower (higher) baseline temperature but higher (lower) mid-Holocene temperature in summer and autumn (winter and spring) compared to the other 14 models.

As shown from the geographical distribution based on the median of the 15 models, the mid-Holocene winter and spring temperatures were reduced by 0.6–2.4 K across China, both with a high consistency of cooling among models (Figs. 3b and 3c). Summer temperature was increased by 0–2.4 K over most of China, except for a cooling over part of the southern Tibetan Plateau and South China, where model consistency was less than 80% (Fig. 3d). In autumn, temperature rose over most of China, with a consistent warming of 0.3–1.8 K over the region west of 110°E but a change smaller than 0.6 K east of 110°E over China (Fig. 3e). As a whole, the large-scale spatial pattern of seasonal temperature changes over China during the mid-Holocene reproduced by the 15 PMIP3 models resembled that simulated by the 36 PMIP1/2 models (Jiang et al., 2012), except in autumn when the simulated magnitude was overall larger for the former than for the latter. The mid-Holocene winter and summer temperature changes over China in the 15-model median were also similar to the 10-model median results in Zheng et al. (2013), except for a weak warming over part of the Tibetan Plateau in winter and a warming across the whole of China in summer for the latter.

During the mid-Holocene winter and spring, SSTs increased slightly at northern high latitudes but decreased with a high consistency among the models over the oceans adjacent to the East Asian continent (Figs. 4b and 4c), leading to an overall cooling over the whole of China in those seasons (Figs. 3b and 3c). Similar to the annual mean, the mid-Holocene summer SSTs increased by 0–1.0 K north of 30°N but decreased by 0–0.6 K south of it, both with a high consistency among models (Fig. 4d), which favored a surface warming over most of China but a slight cooling south of 30°N over China in summer (Fig. 3d). During the mid-Holocene autumn, the 12-model median reproduced generally warmer SSTs in the Northern Hemisphere, contributing to the increased autumn temperature over most of China (Figs. 3e and 4e).

3.3 Model-data comparison

As derived from the 64 records of pollen, lake cores, paleosol, ice cores, peat, sediment, stalagmites, and fossil fruits detailed in Jiang et al. (2012), the mid-Holocene annual temperature over China was reconstructed to be warmer than today. In addition, a number of datasets of pollen samples from paleovegetation have all indicated warmer winter temperatures over China during the mid-Holocene (Yu et al., 2000; Ni et al., 2010), which was even stronger than the annual warming (Xu et al., 1988; Kong et al., 1990; Shi et al., 1993; Guiot et al., 2008; Jiang et al., 2010). Contrary to the reconstruction, colder-than-baseline annual (winter) climate was reproduced by 14 (15) of the 15 PMIP3 models, with a cooling of 0.33 K (1.31 K) for the median of the 15 models, averaged over China during the mid-Holocene (Fig. 2). Concerning the spatial pattern changes, the simulated mid-Holocene annual (winter) temperature was consistently colder than the baseline period over most (all) of China in the PMIP3 models (Figs. 3a and 3b). However, a slight warming was reproduced by the median of the 15 PMIP3 models over northern Northeast China, most of Xinjiang, and part of North and central China, with a high consistency among individual models, except for the former region (Fig. 3a), and thus was qualitatively in accordance with proxy data, though the spatial coverage was very sparse over those areas.

Based on the above, a considerable mismatch still exists between proxy data and PMIP3 simulations, as was also the case between the reconstruction and PMIP1/2 simulations (Jiang et al., 2012). On the other hand, as discussed in Jiang et al. (2012), the colder-than-baseline annual and winter climates reproduced by PMIP3 models were mainly attributed to the negative radiative forcing over China during the mid-Holocene, which were consistently robust between the models, albeit with some uncertainties still apparent. Additionally, uncertainty in the proxy data may be another source for the model-data inconsistency. In spite of the robust warmer annual and winter climates over China as derived from multiple proxy data, the mid-Holocene annual temperature was indicated by Guiot et al. (2008) and Bartlein et al. (2011) to be colder in parts of China. Furthermore, Liu et al. (2014) pointed out that the above reconstructions were mainly based on vegetation records, and thus a seasonal bias and precipitation effects cannot be ruled out to reconcile the contradiction between the reconstructed cooling and the simulated warming. Collectively, further study should focus on more reconstruction work as well as climate model improvement, to narrow the spread between proxy data and simulations.

4 Conclusion

The mid-Holocene annual and seasonal temperature changes over China were revisited using the 15 climate models under the latest PMIP3/CMIP5 protocol. Results showed that, with respect to the baseline period, the mid-Holocene changes in annual and seasonal temperatures over China reproduced by the PMIP3 models were similar to the PMIP1/2 simulations in Jiang et al. (2012). Following the mid-Holocene annual and seasonal insolation changes over China, 14 (15) of the 15 PMIP3 models reproduced colder-than-baseline annual (winter and spring) temperature, whereas all (13) of the 15 models simulated warmer summer (autumn) climate over China during that period. Averaged over China for the median of the 15 models, the mid-Holocene changes in annual, winter, spring, summer, and autumn temperature were −0.33 K, −1.31 K, −1.58 K, 1.02 K, and 0.61 K, respectively — similar to those from the 20 PMIP2 coupled models but generally weaker than those from the 16 PMIP1 AGCMs. A considerable mismatch still exists between the reconstructed warming and the simulated cooling in the PMIP3 models for annual and winter temperatures over China during the mid-Holocene, except over northern Northeast China, most of Xinjiang, and part of North and central China, where a slight warming was reproduced by most of the PMIP3 models.

Acknowledgments. We sincerely thank the anonymous reviewers for their insightful comments, which improved the paper. We also thank the climate modeling groups (listed in Table 1) for producing and making available their model output. This research was supported by the National Natural Science Foundation of China (Grant No. 41222034).

References

Bartlein, P., S. Harrison, S. Brewer, et al., 2011: Pollen-based continental climate reconstructions at 6 and 21 ka: A global synthesis, *Climate Dyn.*, **37**, 775–802.

Berger, A. L., 1978: Long-term variations of daily insolation and quaternary climatic changes, *J. Atmos. Sci.*, **35**, 2362–2367.

Braconnot, P., B. Otto-Bliesner, S. Harrison, et al., 2007: Results of PMIP2 coupled simulations of the mid-Holocene and last glacial maximum—Part 1: Experiments and large-scale features, *Climate Past*, **3**, 261–277.

Dallmeyer, A., M. Claussen, and J. Otto, 2010: Contribution of oceanic and vegetation feedbacks to Holocene climate change in monsoonal Asia, *Climate Past*, **6**, 195–218.

Guiot, J., H. B. Wu, W. Y. Jiang, et al., 2008: East Asian Monsoon and paleoclimatic data analysis: A vegetation point of view, *Climate Past*, **4**, 137–145.

Jiang, D., X. Lang, Z. Tian, et al., 2012: Considerable model-data mismatch in temperature over China during the mid-Holocene: Results of PMIP simulations, *J. Climate*, **25**, 4135–4153.

Jiang, W., J. Guiot, G. Chu, et al., 2010: An improved methodology of the modern analogues technique for palaeoclimate reconstruction in arid and semi-arid regions, *Boreas*, **39**, 145–153.

Joussaume, S., K. E. Taylor, P. Braconnot, et al., 1999: Monsoon changes for 6000 years ago: Results of 18 simulations from the Paleoclimate Modeling Intercomparison Project (PMIP), *Geophys. Res. Lett.*, **26**, 859–862.

Kong, Z. C., N. Q. Du, F. S. Shan, et al., 1990: Vegetational and climatic changes in the last 11,000 years in Qinghai Lake—Numerical analysis based on palynology in core QH85-14C, *Mar. Geol. Quat. Geol.* (in Chinese), **10**, 79–90.

Liu, Z., J. Zhu, Y. Rosenthal, et al., 2014: The Holocene temperature conundrum, *Proc. Natl. Acad. Sci. USA*, **111**, E3501–E3505, doi:10.1073/pnas.1407229111.

Liu, Z., S. P. Harrison, J. Kutzbach, et al., 2004: Global monsoons in the mid-Holocene and oceanic feedback, *Climate Dyn.*, **22**, 157–182.

Ni, J., G. Yu, S. P. Harrison, et al., 2010: Palaeovegetation in China during the late Quaternary: Biome reconstructions based on a global scheme of plant functional types, *Palaeogeogr. Palaeoclimatol. Palaeoecol.*, **289**, 44–61.

O'ishi, R., and A. Abe-Ouchi, 2011: Polar amplification in the mid-Holocene derived from dynamical vegetation change with a GCM, *Geophys. Res. Lett.*, **38**, L14702, doi: 10.1029/2011GL048001.

Shi, Y., Z. Kong, S. Wang, et al., 1993: Mid-Holocene climates and environments in China, *Glob. Planet. Change*, **7**, 219–233.

Taylor, K. E., 2001: Summarizing multiple aspects of model performance in a single diagram, *J. Geophys. Res.*, **106**, 7183–7192.

Taylor, K. E., R. J. Stouffer, and G. A. Meehl, 2012: An overview of CMIP5 and the experiment design, *Bull. Amer. Meteor. Soc.*, **93**, 485–498.

Tian, Z., and D. Jiang, 2013: Mid-Holocene ocean and vegetation feedbacks over East Asia, *Climate Past*, **9**, 2153–2171.

Wang, H. J., 1999: Role of vegetation and soil in the Holocene megathermal climate over China, *J. Geophys. Res.*, **104**, 9361–9367.

Wang, H. J., 2002: The mid-Holocene climate simulated by a grid-point AGCM coupled with a biome model, *Adv. Atmos. Sci.*, **19**, 205–218.

Wang, T., and H. J. Wang, 2013: Mid-Holocene Asian summer climate and its responses to cold ocean surface simulated in the PMIP2 OAGCMs experiments, *J. Geophys. Res.*, **118**, 4117–4128.

Wang, T., H. J. Wang, and D. Jiang, 2010: Mid-Holocene East Asian summer climate as simulated by the PMIP2 models, *Palaeogeogr. Palaeoclimatol. Palaeoecol.*, **288**, 93–102.

Wei, J. F., and H. J. Wang, 2004: A possible role of solar radiation and ocean in the mid-Holocene East Asian monsoon climate, *Adv. Atmos. Sci.*, **21**, 1–12.

Wu, J., and X. J. Gao, 2013: A gridded daily observation dataset over China region and comparison with the other datasets, *Chin. J. Geophys.*, **56**, 1102–1111, doi:10.6038/cjg20130406.

Xu, Q. H., S. Y. Chen, Z. C. Kong, et al., 1988: Preliminary discussion of vegetation succession and climatic change since the Holocene in the Baiyangdian Lake district, *Acta Phytoecol. Geobotan. Sinica* (in Chinese), **12**, 143–151.

Yu, G., X. Chen, J. Ni, et al., 2000: Palaeovegetation of China: A pollen data-based synthesis for the mid-Holocene and last glacial maximum, *J. Biogeogr.*, **27**, 635–664.

Zhao, Y., and S. P. Harrison, 2012: Mid-Holocene monsoons: A multi-model analysis of the inter-hemispheric differences in the responses to orbital forcing and ocean feedbacks, *Climate Dyn.*, **39**, 1457–1487.

Zheng, W., B. Wu, J. He, et al., 2013: The East Asian Summer Monsoon at mid-Holocene: Results from PMIP3 simulations, *Climate Past*, **9**, 453–466.

Zheng, Y. Q., G. Yu, S. M. Wang, et al., 2004: Simulation of paleoclimate over East Asia at 6 ka BP and 21 ka BP by a regional climate model, *Climate Dyn.*, **23**, 513–529.

Zhou, B., and P. Zhao, 2010: Modeling variations of summer upper tropospheric temperature and associated climate over the Asian Pacific region during the mid-Holocene, *J. Geophys. Res.*, **115**, D20109, doi:10.1029/2010JD014029.

Zhou, B., and P. Zhao, 2013: Simulating changes of spring Asian-Pacific oscillation and associated atmospheric circulation in the mid-Holocene, *Int. J. Climatol.*, **33**, 529–538.